Nonlinear analysis based optimal design of double-layer grids using enhanced colliding bodies optimization method

A. Kaveh[*1] and M. Moradveisi[2]

[1]*Center of Excellence For Fundamental Studies in Structural Engineering, School of Civil Engineering, Iran University of Science and Technology, Narmak, Tehran -16, Iran*
[2]*Road, Housing and Urban Development Research Center, Tehran P.O. Box 13145-1696, Iran*

Abstract. In this paper an efficient approach is introduced for design and analysis of double-layer grids including both geometrical and material nonlinearities, while the results are compared with those considering material nonlinearity. Optimum design procedure based on Enhanced Colliding Bodies Optimization method (ECBO) is applied to optimal design of two commonly used configurations of double-layer grids. Two ranges of spans as small and big sizes with certain bays of equal length in two directions are considered for each type of square grids. ECBO algorithm obtains minimum weight grid through appropriate selection of tube sections available in AISC Load and Resistance Factor Design (LRFD). Strength constraints of AISC-LRFD specifications and displacement constraints are imposed on these grids.

1. Introduction

Space structures are typical examples of skeleton frameworks, as a rule consisting of a large number of simple modular, prefabricated units, often of standard size and shape, which combine into light, three dimensional structure which are gaining rapid acceptance, not only because their attractiveness and having a greater reserve of strength as compared with the conventional structures, but also because of being more economical to build.

Many researches consider the prominent geometrical, material nonlinearity effects or both of them in the field of space structures.

One of the most important developments in the field of space structures in the recent years has been the evolution various types of double-layer grids. This form of construction is attracting the attention of architects and engineers alike. Double-layer grids are ideally suited for covering exhibition pavilions, assembly halls, swimming pools, hangars, churches, bridge decks and many types of industrial buildings in which large unobstructed areas are required. Present experience shows that in many countries double-layer grids can be completed successfully much cheaper than equivalent conventional systems, providing at the same time additional advantages, such as greater

---

∗Corresponding author, Ph.D., E-mail: alikaveh@iust.ac.ir

rigidity, erection simplicity and possibility of covering larger areas. Double-layer grids are a logical extension of single-layer grid frameworks, consisting of two or more sets of parallel beams, intersecting each other at right or oblique angles and loaded by forces perpendicular to the plane of the framework. Single-layer grids are used for clear spans up to 10 m. For larger spans double-layer grids are more suitable and provide an economical solution for spans up to 100 m. Double-layer grids consist of two plane grids (which are not necessarily of identical layout) forming the top and bottom layers, parallel to each other, and interconnected by vertical or inclined 'web' diagonal members. Double-layer grids belong to the category of skeletal structures and are composed of a large number of straight members interconnected at the nodes. Whereas the single-layer grids are mainly under the action of flexural moments, the component members of double-layer grids are almost exclusively under the action of axial forces, the elimination of bending moments leads to a full utilization of strength of all the elements. As a rule, double-layer grids are highly statically indeterminate and buckling of any compression member under a heavy concentrated load will not lead to collapse of the whole structure (Makowski 1990).

Methods of optimization can be divided into two general categories of gradient-based methods and metaheuristic algorithms. Many of Gradient-based optimization algorithms have difficulties when dealing with large-scale optimization problems. To overcome these difficulties utilizing metaheuristic algorithms is inevitable. The formulation of metaheuristic algorithms is often inspired by either natural phenomena or physical laws. Every metaheuristic algorithm consists of two phases: exploration of the search space and exploitation of the best solutions found. One of the main problems in developing a good metaheuristic algorithm is to keep a reasonable balance between the exploration and exploitation abilities. In the past decades, structural optimization has been studied by using different metaheuristic algorithms (Kaveh 2014) such as genetic algorithm (Erbatur *et al*. 2000), particle swarm optimization (Perez and Behdinan 2007), ant colony optimization (Camp *et al*. 2005), charged system search (Kaveh and Talatahari 2010a), harmony search (Degertekin 2012), flower pollination (Bekdaş *et al*. 2015), teaching-learning-based optimization (Degertekin and Hayalioglu 2013), Water Cycle, Mine Blast and improved mine blast algorithms (Sadollah *et al*. 2015), Search Group Algorithm (Gonçalves *et al*. 2015), Ant Lion Optimizer (Mirjalili 2015), and dolphin monitoring for enhancing metaheuristic algorithms (Kaveh and Farhoudi 2016), are other metaheuristic algorithms which have sources in nature. Colliding Bodies Optimization (CBO) is a new metaheuristic search algorithm that is developed by Kaveh and Mahdavi (Kaveh and Mahdavi 2015). CBO is based on the governing laws of one dimensional collision between two bodies from the physics that one object collides with other object and they move toward minimum energy level. The CBO is simple in concept, depends on no internal parameters, and does not use memory for saving the best-so-far solutions. The Enhanced Colliding Bodies Optimization (ECBO) is introduced by Kaveh and Ilchi Ghazaan (Kaveh and Ilchi Ghazaan 2014) and it uses memory to save some historically best solution to improve the CBO performance without increasing the computational cost. In this method, some components of agents are also changed to jump out from local minima. Some other applications of metaheuristic algorithms can be found in (Gholizadeh and Milany 2016).

This study focuses on economical and performance comparison of two commonly used double-layer grid configurations, namely two-way on two-way grids and diagonal on diagonal grids. The span ranges of 12×12 m and 30×30 m with certain bays of equal length in two directions are considered as small and big size grids, respectively. Many publication and researches have considered the influence of nonlinearities of space structures (Code of Practice for Space Structures. 2010, Koushky *et al*. 2009, Saka and Ulker 1991, Kaveh and Talatahari 2010b, Saka

2007) and it is observed that some of those have nonlinear behavior even in usual range of loading (Kaveh and Rezaei 2015, Kaveh and Talatahari 2011). Therefore, neglecting nonlinear effects in design optimization of these structures may led to uneconomic designs and for this reason in the case of nonlinear optimization, geometrical and material nonlinearity effects are taken into account. On the other hand, as a result of the developments in structural optimization techniques, the structures are designed more and more lighter which makes them sensitive to any sort of imperfections. These structures require nonlinear analysis to obtain their behavior under external loadings. Therefore, design examples are provided to illustrate the contrasts between the material and both material and geometrical nonlinearity behavior during the nonlinear analysis of structures.

2. Optimum design of double-layer grids

The allowable cross sections are considered as 37 steel pipe sections shown in Table 1, where the abbreviations ST, EST, and DEST stand for standard weight, extra strong, and double extra strong, respectively. These sections are taken from AISC-LRFD (AISC-LRFD. 2011) which is also utilized as the code of design.

Table 1 The allowable steel pipe sections taken from AISC-LRFD

	Type	Nominal diameter (in)	Weight per *ft* (lb)	Area (in^2)	*I* (in^4)	Gyration radius (in)	*J* (in^4)
1	ST	½	0.85	0.25	0.017	0.261	0.034
2	EST	½	1.09	0.32	0.02	0.25	0.04
3	ST	¾	1.13	0.333	0.037	0.334	0.074
4	EST	¾	1.47	0.433	0.045	0.321	0.09
5	ST	1	1.68	0.494	0.087	0.421	0.175
6	EST	1	2.17	0.639	0.106	0.407	0.211
7	ST	1 ¼	2.27	0.669	0.195	0.54	0.389
8	ST	1 ½	2.72	0.799	0.31	0.623	0.62
9	EST	1 ¼	3.00	0.881	0.242	0.524	0.484
10	ST	2	3.65	1.07	0.666	0.787	1.33
11	EST	1 ½	3.63	1.07	0.391	0.605	0.782
12	EST	2	5.02	1.48	0.868	0.766	1.74
13	ST	2 ½	5.79	1.7	1.53	0.947	3.06
14	ST	3	7.58	2.23	3.02	1.16	6.03
15	EST	2 ½	7.66	2.25	1.92	0.924	3.85
16	DEST	2	9.03	2.66	1.31	0.703	2.62
17	ST	3 ½	9.11	2.68	4.79	1.34	9.58
18	EST	3	10.25	3.02	3.89	1.14	8.13
19	ST	4	10.79	3.17	7.23	1.51	14.5
20	EST	3 ½	12.50	3.68	6.28	1.31	12.6
21	DEST	2 ½	13.69	4.03	2.87	0.844	5.74

Table 1 Continued

22	ST	5	14.62	4.3	15.2	1.88	30.3
23	EST	4	14.98	4.41	9.61	1.48	19.2
24	DEST	3	18.58	5.47	5.99	1.05	12
25	ST	6	18.97	5.58	28.1	2.25	56.3
26	EST	5	20.78	6.11	20.7	1.84	41.3
27	DEST	4	27.54	8.1	15.3	1.37	30.6
28	ST	8	28.55	8.4	72.5	2.94	145
29	EST	6	28.57	8.4	40.5	2.19	81
30	DEST	5	38.59	11.3	33.6	1.72	67.3
31	ST	10	40.48	11.9	161	3.67	321
32	EST	8	43.39	12.8	106	2.88	211
33	ST	12	49.56	14.6	279	4.38	559
34	DEST	6	53.16	15.6	66.3	2.06	133
35	EST	10	54.74	16.1	212	3.63	424
36	EST	12	65.42	19.2	362	4.33	723
37	DEST	8	72.42	21.3	162	2.76	324

ST=Standard weight, EST=Extra strong, DEST=Double extra strong

The aim of optimizing the grid weight is to find a set of design variables that has the minimum weight satisfying certain constraints. This can be expressed as

$$\text{Find } \{X\} = [x_1, x_2, x_3, ..., x_{ng}], x_i \in D = \{d_1, d_2, d_3, ..., d_{37}\}$$

$$\text{To minimize } W(\{X\}) = \sum_{i=1}^{ng} x_i \sum_{j=1}^{nm(i)} \rho_j . L_j \tag{1}$$

where $\{X\}$ is the set of design variables; ng is the number of member groups in structure (number of design variables); D is the cross-sectional areas available for groups according to Table 1; $W(\{X\})$ presents weight of the grid; $nm(i)$ is the number of members for the ith group; ρ_j and L_j denote the material density and the length for the jth member of the ith group, respectively.

The constraint conditions for grid structures are briefly explained in the following:

Displacement constraints

$$\delta^i \leq \delta^{max}, i = 1, 2, ..., nn \tag{2}$$

Tension member constraints:

$$P_u \leq P_r: \qquad P_r = min \begin{cases} F_y . A_g . \emptyset_t \\ F_u . A_e . \emptyset_t \end{cases} \qquad \begin{matrix} \emptyset_t = 0.9 \\ \emptyset_t = 0.75 \end{matrix} \tag{3}$$

Compression member constraints:

$$P_u \leq P_r \qquad , P_r = \emptyset_c . F_{cr} . A_g; \quad \emptyset_c = 0.9$$

$$F_{cr} = min \begin{cases} (0.658^{F_y/F_e}) F_y \\ 0.877 F_e \end{cases} , \quad \begin{matrix} \frac{KL}{r} \leq 4.71 \sqrt{E/F_y} \\ \frac{KL}{r} > 4.71 \sqrt{E/F_y} \end{matrix} , \quad F_e = \pi^2 E / (KL/r)^2 \tag{4}$$

Slenderness ratio constraints:

$$\begin{aligned} \lambda_c &= KL/r \leq 200 \quad \text{for compression members} \\ \lambda_t &= KL/r \leq 300 \quad \text{for tension members} \end{aligned} \tag{5}$$

where δ^i and δ_i^{max} are the displacement and allowable displacement for the ith node; nn is the number of nodes; nm is the total number of members and K is effective length factor taken equal to 1; P_u is the required strength (tension or compression); A_g and A_e cross sectional and effective net area of a member, respectively.

In order to handle the constraints, a penalty approach is utilized. In this method the aim of the optimization is redefined by introducing the cost function as

$$f_{cost}(\{X\}) = (1 + \epsilon_1 . v)^{\epsilon_2} \times W(\{X\}), v = \sum_{i=1}^{nn} v_i^d + \sum_{i=1}^{nm} \left(v_i^\sigma + v_i^\lambda \right) \tag{6}$$

where v is the constraint violation function; v_i^d, v_i^σ and v_i^λ are constraint violation for displacement, stress and slenderness ratio, respectively. ϵ_1 and ϵ_2 are penalty function exponents which are selected considering the exploration and exploitation rate of the search space. Here ϵ_1 is set to unity; and in the first steps of the search process, ϵ_2 is set to 1 and ultimately increased to 3. Such a scheme penalizes the unfeasible solutions more severely as the optimization process proceeds. As a result, in the early stages the agents are free to explore the search space, but at the end they tend to choose solutions with no violation.

3. ECBO algorithm

Colliding bodies optimization (CBO) is a new population-based stochastic optimization algorithm based on the governing laws of one dimensional collision between two bodies from the physics (Kaveh and Mahdavi 2014). Each agent is modeled as a body with a specified mass and velocity. A collision occurs between pairs of objects to find the global or near-global solutions. Enhanced colliding bodies optimization (ECBO) uses memory to save some best solutions and utilizes a mechanism to escape from local optima (Kaveh and Ilchi Ghazaan 2014).

3.1 A brief explanation and formulation of the main algorithm (CBO)

In CBO, each solution candidate X_i containing a number of variables (i.e., $X_i = \{X_{i,j}\}$) is considered as a colliding body (CB). The massed objects are composed of two main equal groups: stationary and moving objects, where the moving objects move to follow stationary objects and a collision occurs between pairs of objects (Fig. 1). This is done for two purposes: (I) to improve the positions of moving objects and (II) to push stationary objects towards better positions. After the collision, new positions of colliding bodies are updated based on new velocity by using the collision laws governed by the laws of momentum and energy (Kaveh and Mahdavi 2015). When a collision occurs in an isolated system, the total momentum of the system of objects is conserved. Provided that there are no net external forces acting upon the objects, the momentum of all objects before the collision equals the momentum of all objects after the collision.

CBO starts with an initial population consisting of $2n$ parent individuals created by means of a random initialization. Then, CBs are sorted in ascending order based on the value of cost function
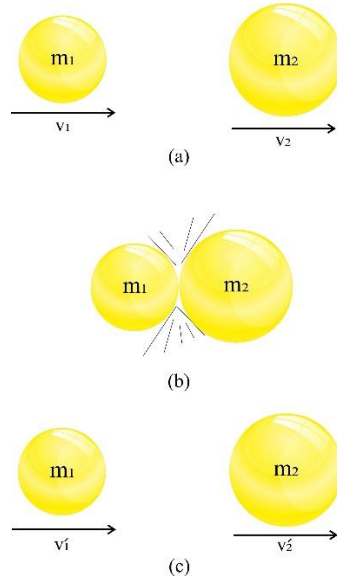
Fig. 1 Collision between two bodies, (a) before collision, (b) same time collision and (c) after collision
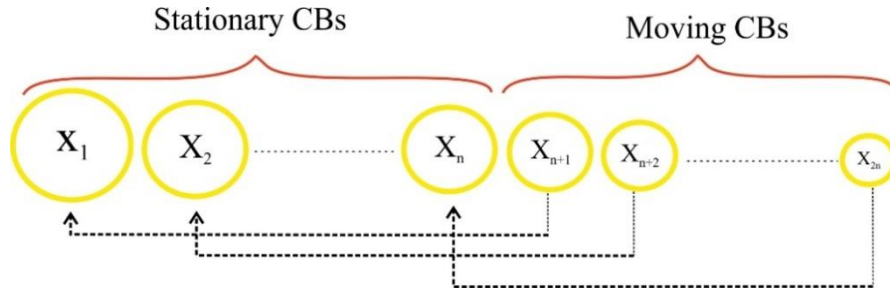

Fig. 2 The sorted CBs in an ascending order and the mating process for the collision

as shown in Fig. 2.

The CBO procedure can briefly be outlined as follows:

As stated before each agent called CB has specified mass, that is defined as

$$m_k = \frac{\dfrac{1}{fit(k)}}{\sum_{i=1}^{n} \dfrac{1}{fit(i)}}, \quad k = 1,2,\dots,n \tag{7}$$

where *fit*(*i*) represents the objective function value of the *i*th CB and *n* is the number of colliding bodies. After sorting colliding bodies according to their objective function values in an increasing order, two equal groups are created: (I) stationary group, (II) moving group (Fig. 2). Moving objects collide to stationary objects to improve their positions and push stationary objects towards better positions. The velocities of the stationary and moving bodies before collision (v_i) are calculated by

$$v_i = 0, \quad i = 1,\dots,\frac{n}{2} \tag{8}$$

$$v_i = x_{i-\frac{n}{2}} - x_i, \quad i = \frac{n}{2} + 1, \frac{n}{2} + 2 \ldots, n \tag{9}$$

where x_i is the position vector of the ith CB. The velocity of stationary and moving CBs after the collision (v_i') are evaluated by

$$v_i' = \frac{\left(m_{i+\frac{n}{2}} + \varepsilon m_{i+\frac{n}{2}}\right) v_{i+\frac{n}{2}}}{m_i + m_{i+\frac{n}{2}}} \qquad i = 1,2,\ldots,\frac{n}{2} \tag{10}$$

$$v_i' = \frac{\left(m_i - \varepsilon m_{i-\frac{n}{2}}\right) v_i}{m_i + m_{i-\frac{n}{2}}} \qquad i = \frac{n}{2} + 1, \frac{n}{2} + 2, \ldots, n \tag{11}$$

$$\varepsilon = 1 - \frac{iter}{iter_{max}} \tag{12}$$

where ε is the coefficient of restitution (COR), *iter* and *iter$_{max}$* are the current iteration number and the total number of iteration for optimization process, respectively. New positions of each group are stated by the following formulas.

$$x_i^{new} = x_i + rand_\text{o} v_i', \qquad i = 1,2,\ldots,\frac{n}{2} \tag{13}$$

$$x_i^{new} = x_{i-\frac{n}{2}} + rand_\text{o} v_i', \quad i = \frac{n}{2} + 1, \ldots, n \tag{14}$$

where x_i^{new}, x_i and v_i' are the new position, previous position and the velocity after the collision of the ith CB, respectively. *rand* is a random vector uniformly distributed in the range of [-1,1] and the sign "$_\text{o}$" denotes an element-by-element multiplication.

3.2 Pseudo-code of the ECBO algorithm

In the enhanced colliding bodies optimization (ECBO), a memory that saves a number of historically best CBs is utilized to improve the performance of the CBO and reduce the computational cost. Furthermore, ECBO changes some components of CBs randomly to prevent premature convergence (Kaveh and Ilchi Ghazaan 2015). In this section, in order to introduce the ECBO algorithm the following steps should be taken.

3.2.1 Initialization
Step 1: The initial locations of CBs are created randomly in an *m*-dimensional search space.

$$x_i^0 = x_{min} + random_\text{o}(x_{max} - x_{min}), \quad i = 1,2,3,\ldots,n \tag{15}$$

where x_i^0 is the initial solution vector of the ith CB. x_{min} and x_{max} are the minimum and the maximum allowable variables vectors; and random is a random vector with each component being in the interval [0,1].

3.2.2 Search
Step 1: The value of the mass for each CB is calculated by Eq. (7).

Step 2: Colliding Memory (CM) is considered to save some historically best CB vectors and their related mass and objective function values. The size of the CM is taken as $n/10$ (n is the number of the population size) in this study. At each iteration, solution vectors that are saved in the CM are added to the population and the same number of the current worst CBs are deleted.

Step 3: CBs are sorted according to their objective function values in an increasing order. To select the pairs of CBs for collision, they are divided into two equal groups: (I) stationary group, (II) moving group.

Step 4: The velocities of stationary and moving bodies before collision are evaluated by Eqs. (8) and (9), respectively.

Step 5: The velocities of stationary and moving bodies after collision are calculated by Eqs. (10) and (11), respectively.

Step 6: The new location of each CB is evaluated by Eqs. (13) or (14).

Step 7: A parameter like ***Pro*** within (0, 1) is introduced and specified whether a component of each CB must be changed or not. For each CB ***Pro*** is compared with rn_i (i=1,2,…,n) which is a random number uniformly distributed within (0, 1). If rn_i <***Pro***, one dimension of ith CB is selected randomly and its value regenerated by

$$x_{ij} = x_{j,min} + random.\left(x_{j,max} - x_{j,min}\right) \tag{16}$$

where x_{ij} is the jth variable of the ith CB. $x_{j,min}$ and $x_{j,max}$ are the lower and upper bounds of the jth variable. In this paper, the value of ***Pro*** set to 0.3.

3.2.3 Terminating condition check

Step 1: After the predefined maximum evaluation number, the optimization process is terminated.

4. Nonlinear analysis

Nonlinear static analysis is a procedure in which the magnitude of the structural loading is incrementally increased in accordance with a certain predefined pattern. The use of nonlinear static procedures, is inevitably going to be favored over complex, impractical for widespread professional use, nonlinear time-history methods. The procedure consists of an incremental-iterative solution of the static equilibrium equations corresponding to a nonlinear structural model subjected to a monotonically increasing vertical load pattern. The structural resistance is evaluated and the stiffness matrix is updated at each increment of the forcing function, up to convergence. The solution proceeds until (I) a predefined performance limit state is reached, (II) structural collapse is incipient or (III) the programs fails to converge. Nonlinear static analysis load cases can be force controlled, or they can be displacement controlled. Both the force distribution and target displacement are based on assumptions that the response is controlled by the fundamental mode and the mode shape remains unchanged until collapse occurs. It would seem that applying displacement loading, rather than force action would be an appropriate option in nonlinear static analysis procedures. In this study the displacement control load case is taken into account during the nonlinear analysis while the central node of the grid is considered as the control node. Gravity loads are applied to the structure first, and vertical loads are then applied in an incremental fashion. The target displacement is intended to represent the maximum displacement likely to be experienced while the analysis is carried out up to failure, thus it enables determination of collapse
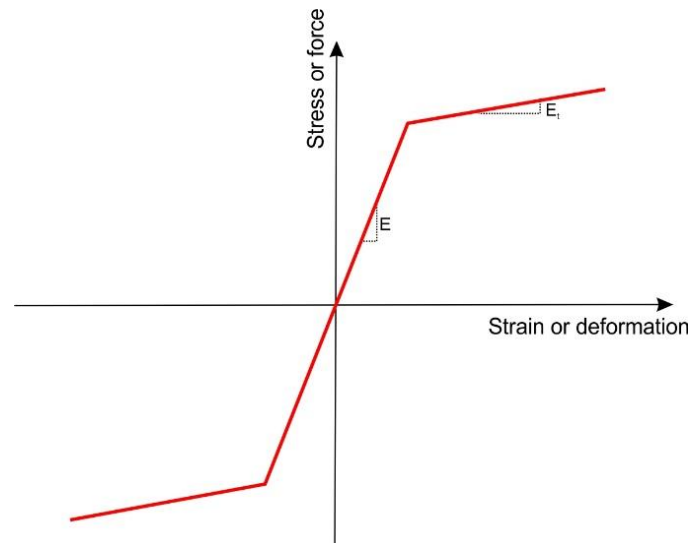
Fig. 3 The stress-strain relationship of a uniaxial bilinear steel material

load and ductility capacity. The vertical inelastic forces versus displacement response for the complete structure is analytically computed. This type of analysis enables weakness in the structure to be identified. The performance of nonlinear static analysis primarily depends upon choice of material models, thus a uniaxial bilinear steel material with kinematic hardening is taken into account exist in OpenSees (2011) platform as shown in Fig. 3. The strain-hardening ratio (ratio between post-yield tangent and elastic tangent) is equal to 0.01.

Here, a bi-linear behavior for double layer grid elements both in tension and comparison. One can also consider an element with plasticity and large deflection capabilities according to FEMA-274 for including the effects of buckling in element behavior, as in Gholizadeh (2016).

5. Structural models

Two commonly used configurations for double-layer grids considered in this study are two-way on two-way and diagonal on diagonal square grids (Makowski 1990). Two ranges of spans 12×12 m and 30×30 m with certain bays of equal length in two directions are considered as small and big size spans, respectively. Simply supported condition is employed for bottom layer at the corner nodes. The uniformity of the distribution of stiffness in the vicinity of the structure is an important issue for large-scale structures. If part of the structure has elements of low axial forces and small displacements (low cross sections), and another part contains elements of high cross sections, then the uniformity of the distribution of the stiffness will not be achieved. For this reason, the elements grouping is selected according to two symmetry lines of the configuration and leads to uniform distribution of stiffness in whole structure. Therefore, elements at top layer, bottom layer, and diagonal elements are put into different groups in a square-like manner around central node (Kaveh *et al*. 2011). Due to symmetry, only a quarter of the grids are shown in Figures.
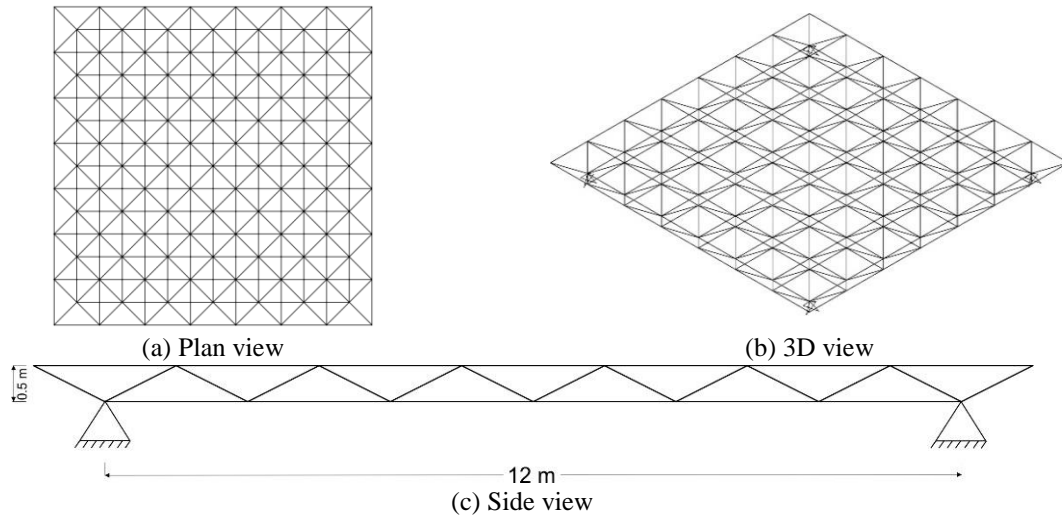
(a) Plan view   (b) 3D view

(c) Side view

Fig. 4 Schematic of a 12×12m two-way on two-way grid

(a) Plan view   (b) 3D view
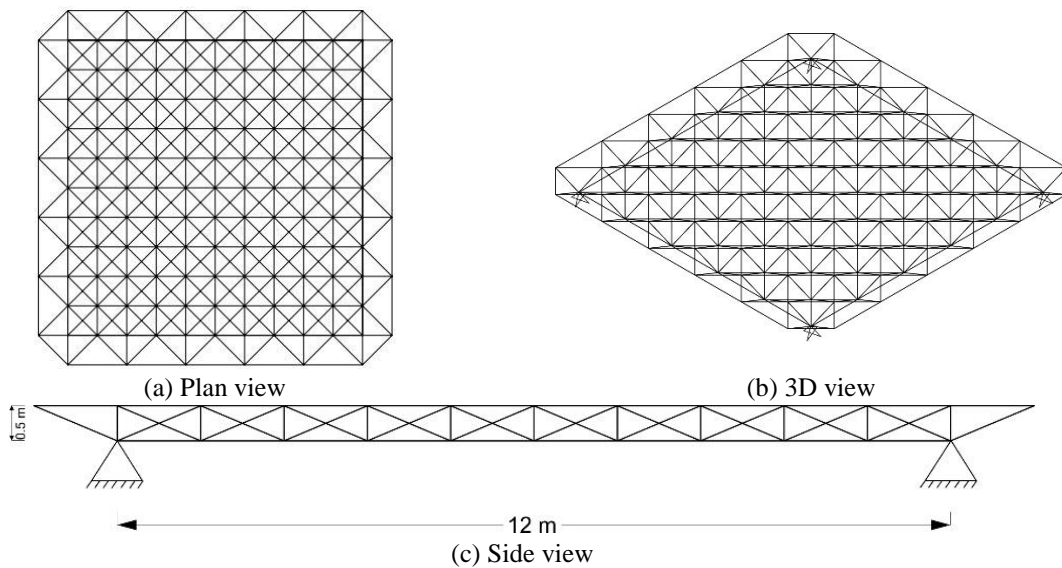

12 m

(c) Side view

Fig. 5 Schematic of a 12×12 m diagonal on diagonal grid

6. The numerical examples

The double-layer grids are assumed as ball-jointed, and top-layer joints are subjected to concentrated vertical loads transmitted from the uniformly distributed load of 200 kg/m^2 according to load bearing areas of top layer joints. Stress and slenderness constraints (Eqs. (3), (4) and (5)) according to AISC-LRFD provisions, and displacement limitations of span/240 were imposed on all nodes in vertical direction. The modulus of elasticity and tangent modulus of elasticity is considered as 200 kN/mm^2 (29000 ksi) and 2 kN/mm^2 (290 ksi), respectively. The yield stress of steel is taken as 248.2 MPa (36 ksi).

In ECBO algorithm, the population of $n=30$ CBs is utilized, and the size of colliding memory is considered as $n/10$ that is taken as 3. The predefined maximum evaluation number is considered as 9,000 analysis for all examples. In all problems, CBs are allowed to select discrete values from the permissible list of cross sections (real numbers are rounded to the nearest integer in each iteration).

Example 1: A 12× 12 m double-layer square grid

A 12×12 m span case is studied as the small size of double-layer grids. The first common type is the two-way on two-way grid which contains 113 nodes and 392 members, and the second one is the diagonal on diagonal grid with 145 nodes and 528 members. The schematic of the grids are shown in Fig. 4 and Fig. 5, respectively. Grouping patterns lead to 15 and 17 design variables for two-way on two-way and diagonal on diagonal grids, respectively as depicted in Fig. 6. Thus, there are two size optimization problems with 15 and 17 variables. Table 2 shows the best design vectors and the corresponding weights for two types of double-layer grids. It can be observed that two-way on two-way grid is economical choice for covering small span cases but if the height of the structure is flexible to choose (Geometry optimization) the diagonal on diagonal is suitable form for small span length than two-way on two-way grid even with larger number of members. In general the fundamental difference between diagonal and rectangular grids is that in the former the beams are of varying length (L) and therefore if all the beams are of the same cross-sectional dimensions and have the same axial stiffness (EA), their relative stiffness (EA/L) varies considerably. The diagonal grid consists of beams forming an oblique angle with the walls. From Table 2, it can be concluded that ECBO can find the weight for two-way on two-way grid which is

Table 2 Optimum design of 12×12m double-layer grids

Group number	Optimum section (designations)	
	ECBO algorithm	
	Two-way on two-way grid	Diagonal on diagonal grid
1	PIPST (2 ½)	PIPST (6)
2	PIPST (¾)	PIPST (3)
3	PIPST (3)	PIPEST (1 ½)
4	PIPST (3)	PIPEST (2 ½)
5	PIPEST (2 ½)	PIPEST (2 ½)
6	PIPST (2 ½)	PIPEST (2)
7	PIPST (1 ¼)	PIPEST (1)
8	PIPST (1)	PIPEST (¾)
9	PIPST (¾)	PIPST (1 ¼)
10	PIPST (2 ½)	PIPST (2)
11	PIPEST (¾)	PIPST (½)
12	PIPEST (1 ½)	PIPST (3 ½)
13	PIPEST (2)	PIPEST (1 ½)
14	PIPDEST (2)	PIPST (1 ¼)
15	PIPST (3)	PIPEST (1 ½)
16	N/A	PIPEST (2)
17	N/A	PIPST (6)
Best Weight (kg)	4771.50	6686.87

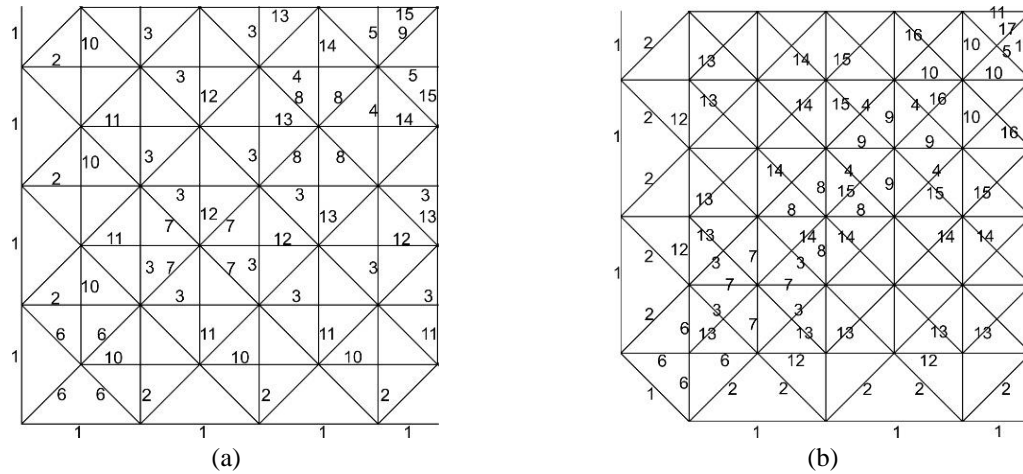(a)   (b)

Fig. 6 Element grouping of a 12×12 m (a) Two-way on two-way grid, (b) Diagonal on diagonal grid
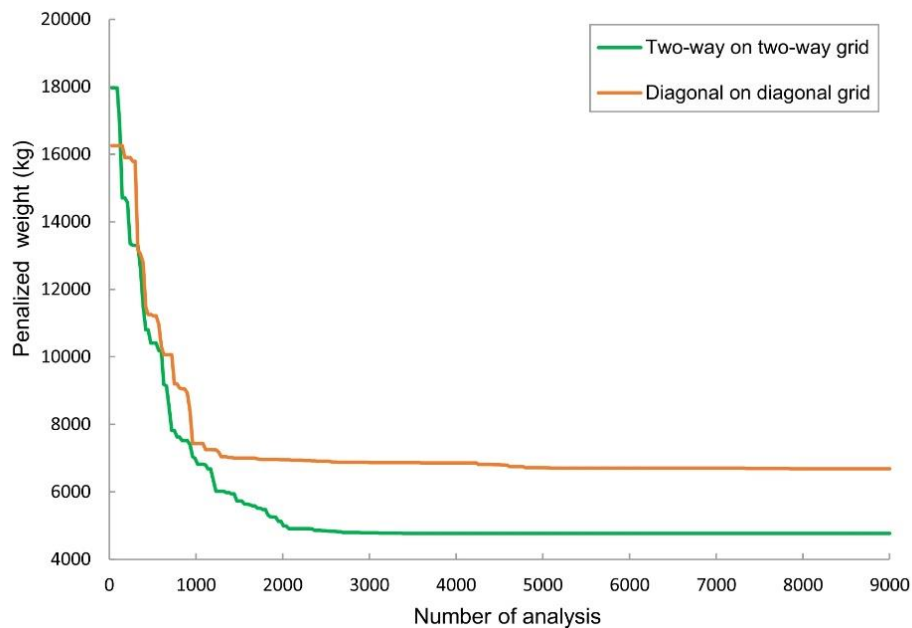

Fig. 7 Convergence curves obtained for the 12×12m double-layer grids

1915.37 kg (28.64%) lighter than diagonal on diagonal grid. For graphical comparison of two types of grids, Fig. 7 illustrate the convergence curve for both of them.

For performance comparison of the grids, the nonlinear analysis was carried out and the results are compared. The nonlinear analysis procedure was implemented in two phases. First the only material nonlinearity was taken into account according to the diagram which is shown in Fig. 8, and in the second phase both material and geometrical nonlinearity (fully nonlinear analysis) was implemented for considering the realistic behavior of the structures. The fully nonlinear analysis continued up to reaching the point of total (global) collapse.
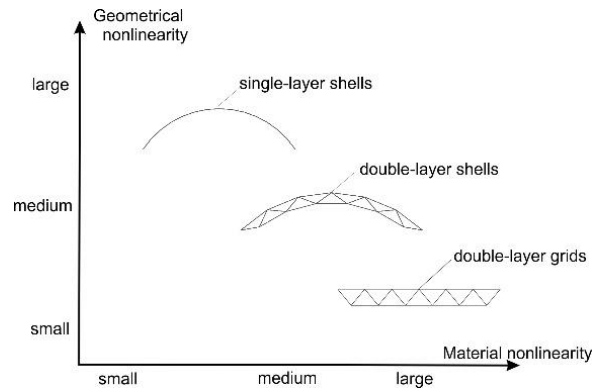
Fig. 8 Effects of nonlinearities (Code of Practice for Space Structures 2010)
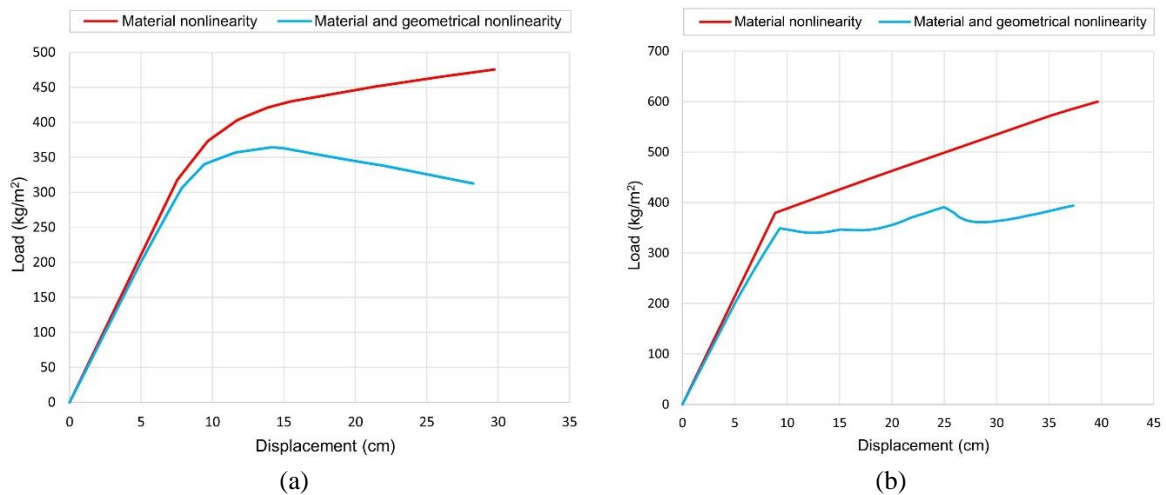

| (a) | (b) |

Fig. 9 Capacity curves of the 12×12 m (a) two-way on two-way grid, (b) diagonal on diagonal grid

In Figs. 9(a) and 9(b) the capacity curves are shown for the two-way on two-way grid and diagonal on diagonal grid, respectively. With these figures the nonlinear static response of the grids could be investigated from the initial elastic to the highly nonlinear and even the degrading stages. The significant differences are evident among the only material nonlinear analysis and fully nonlinear analysis, thus geometrical nonlinearity playing the important role during the nonlinear analysis procedure. Such differences are more pronounced in two-way on two-way grid and lead to degrading the capacity curve. In the comparison of the two types of double-layer grids, two-way on two-way elements are failed consecutively and show the better stress distribution between the members, for this reason capacity curves are smooth. In the diagonal on diagonal grid some of the members are failed simultaneously whereby the stiffness of whole structure decreased abruptly at the yield point. As stated before, double layer grids are highly statically indeterminate and buckling of any compression member under a heavy concentrated load will not lead to collapse of whole structure. This advantage is completely evident through the curves. Particularly, according to the Fig. 9(b) blue curve (fully nonlinear analysis) in the diagonal on diagonal grid, failure of some members do not lead to collapse of entire structure and when the load bearing capacity of

these members are significantly decreased, the stress ratio of the low forced members are increased due to indeterminacy. It is also worthwhile to mention that the ultimate strength of two-way on two-way grid which is obtained by fully nonlinear analysis is 364 kg/m^2 while for diagonal on diagonal grid this value is equal to 394 kg/m^2 because of its greater rigidity leads to substantial reduction in the deflections and without considering number and complexity of joints, diagonal on diagonal grid is often favored by engineers and architects because of its convenience and appealing features.

Example 2: A 12× 12 m square on larger square grid

In this case the 12×12 m square on larger square double-layer grids is considered as the second test problem. First type is two-way on larger two-way grid contains 109 nodes and 360 members and second type is diagonal on larger diagonal grid contains 133 nodes and 432 members. Each type has some openings at the middle of the grid created by removing some of the bottom layer members (usually in tension) and the attached bracings of the square on square offset at a rectangular pattern. For better comparison, the geometry of the grids are selected as the same with usual type which is investigated in previous section. Due to the addition of the openings, this system is more suitable when the architect intends to provide more natural lights inside the building (skylights can be placed within the openings). This system is usually selected for structures subjected to normal range of loads. The uniformly distributed load of 200 kg/m^2 is transmitted to the concentrated vertical loads which are assigned to the nodes of the top grid in the proportion of their load bearing area, and also to obtain a practical structure is considered. Figs. 10 and 11 show the schematic of the two-way on larger two-way grid and diagonal on larger diagonal grid, respectively.

Both diagonal and top layer elements grouping is following the pattern as shown in Fig. 6 and the only bottom layer element grouping is differ from last section, for this reason and for better understanding of which elements of bottom layer are removed to create these configurations, the
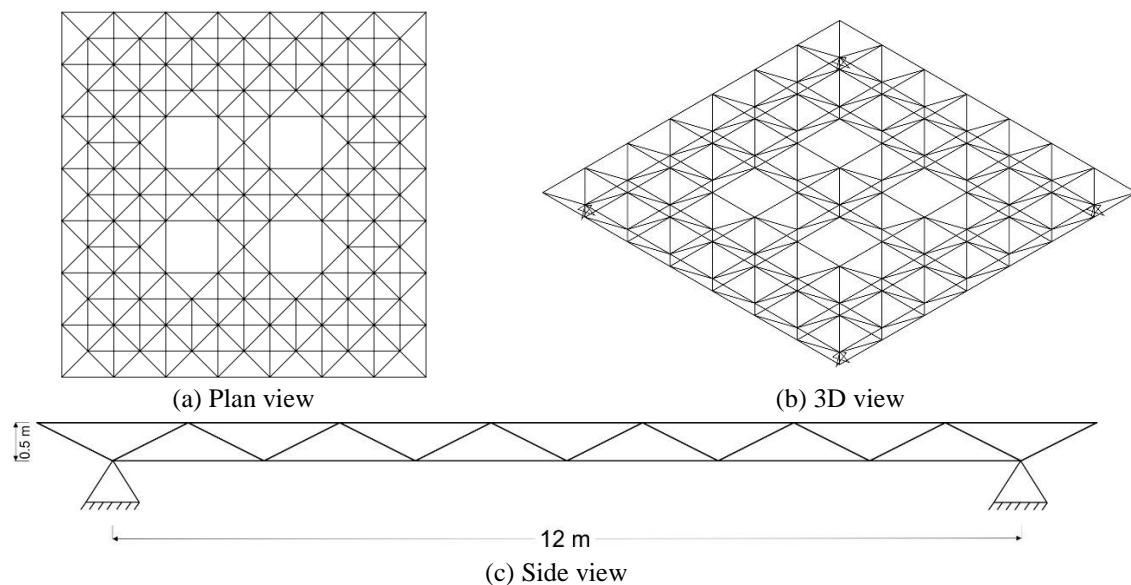

(a) Plan view	(b) 3D view

0.5 m

12 m

(c) Side view

Fig. 10 Schematic of a 12×12 m two-way on larger two-way grid

(a) Plan view   (b) 3D view
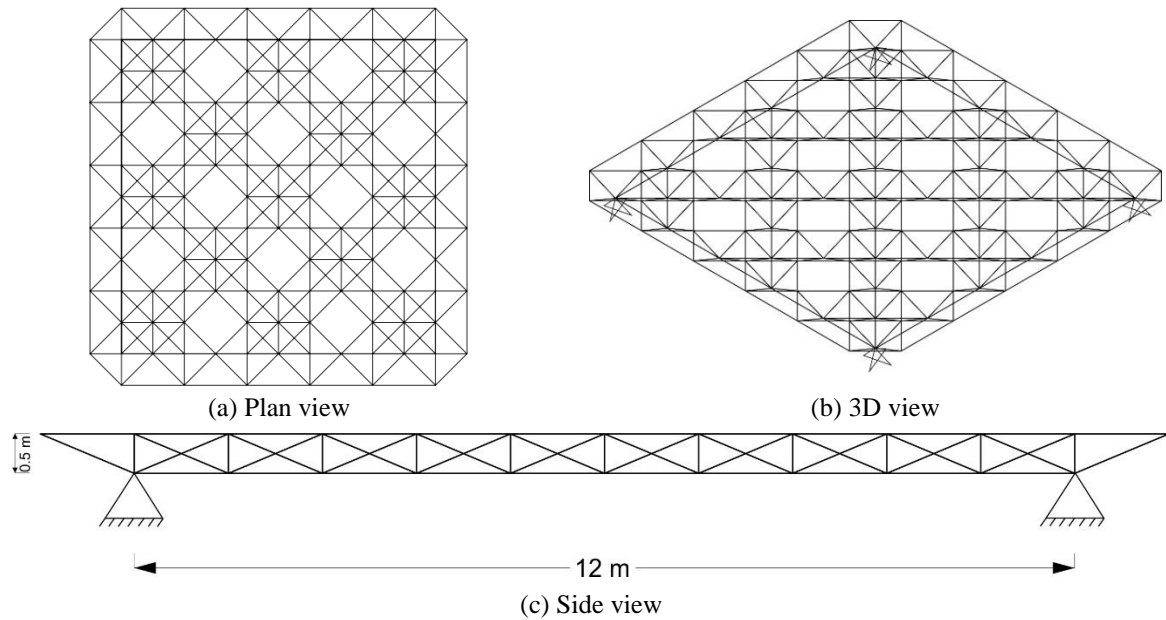
(c) Side view

Fig. 11 Schematic of a 12×12 m diagonal on larger diagonal grid
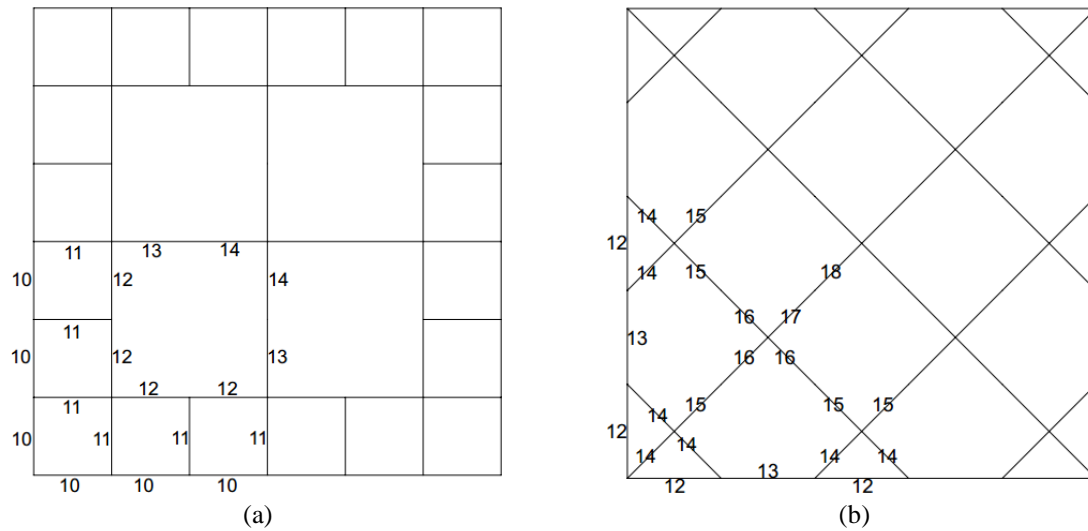

(a)   (b)

Fig. 12 Element grouping of 12×12 m bottom layer (a) Two-way on larger two-way grid, (b) Diagonal on larger diagonal grid

only element grouping of bottom layer is depicted in Fig. 12. The 360 members of two-way on larger two-way grid are categorized into 14 groups and for diagonal on larger diagonal grid all 432 members are divided into 18 groups. The optimization results are presented in Table 3. The proposed method obtained 4879.96 kg and 6672.21 kg for two-way on larger two-way grid and daigonal on larger diagonal grid, respectively. The optimization results shown that two-way on larger two-way grid is 1792.25 kg (26.9%) lighter than diagonal on larger diagonal grid and it is an

Table 3 Optimum design of 12×12 m square on larger square double-layer grids

Group number	Optimum section (designations)	
	ECBO algorithm	
	Two-way on larger two-way grid	Diagonal on larger diagonal grid
1	PIPEST (2)	PIPDEST (4)
2	PIPST (¾)	PIPST (2 ½)
3	PIPST (3 ½)	PIPEST (1 ½)
4	PIPEST (2 ½)	PIPST (2 ½)
5	PIPDEST (2)	PIPEST (4)
6	PIPST (2 ½)	PIPEST (2)
7	PIPST (1 ½)	PIPST (1 ¼)
8	PIPST (1 ¼)	PIPST (1)
9	PIPST (¾)	PIPEST (1 ½)
10	PIPST (2 ½)	PIPEST (1)
11	PIPST (¾)	PIPST (½)
12	PIPST (2 ½)	PIPEST (3)
13	PIPEST (2 ½)	PIPST (1 ¼)
14	PIPDEST (3)	PIPEST (1 ½)
15	N/A	PIPEST (1 ½)
16	N/A	PIPEST (2 ½)
17	N/A	PIPEST (4)
18	N/A	PIPEST (5)
Best Weight (kg)	4879.96	6672.21

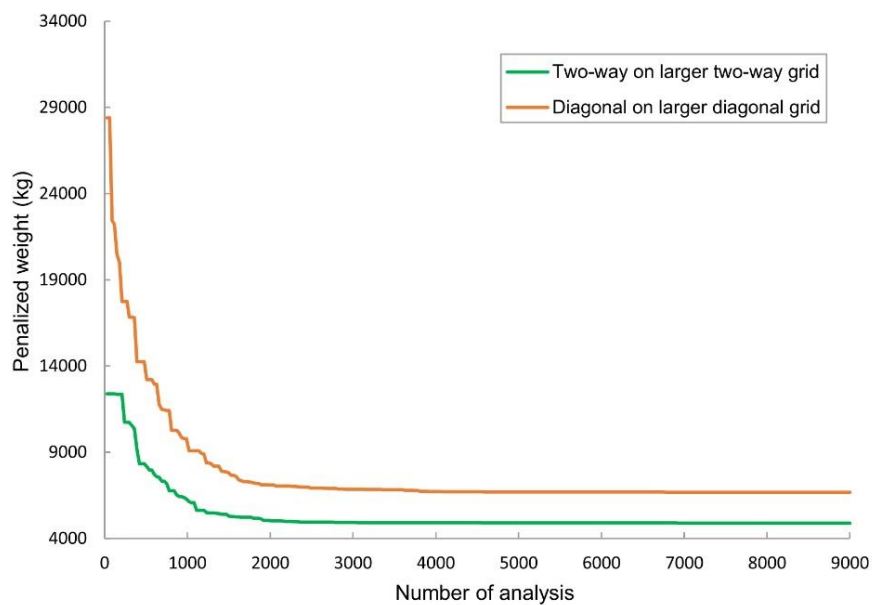Fig. 13 Convergence curves obtained for the 12×12 m square on larger square double-layer grids
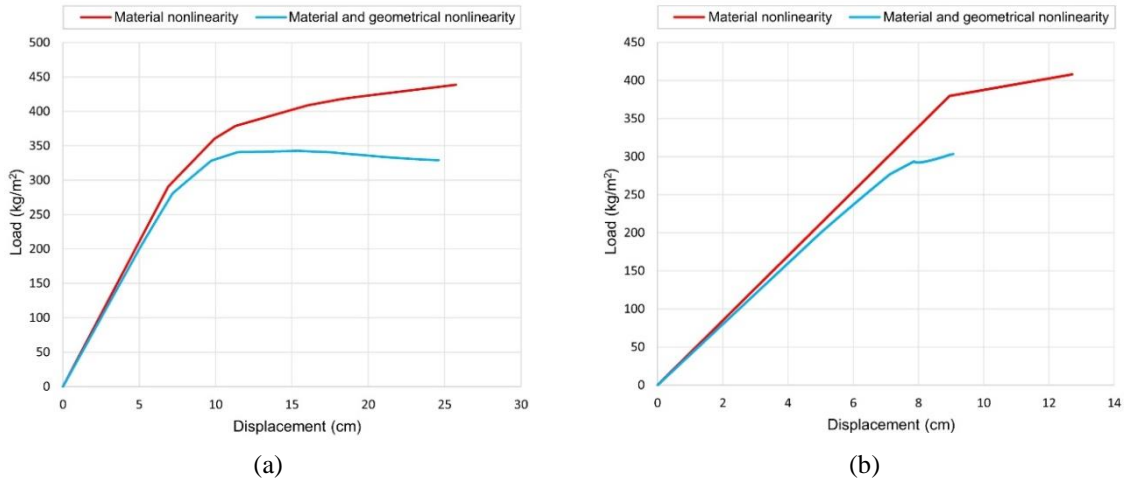
(a)   (b)

Fig. 14 Capacity curves of the 12×12 m (a) two-way on larger two-way grid, (b) diagonal on larger diagonal grid

(a) Plan view   (b) 3D view
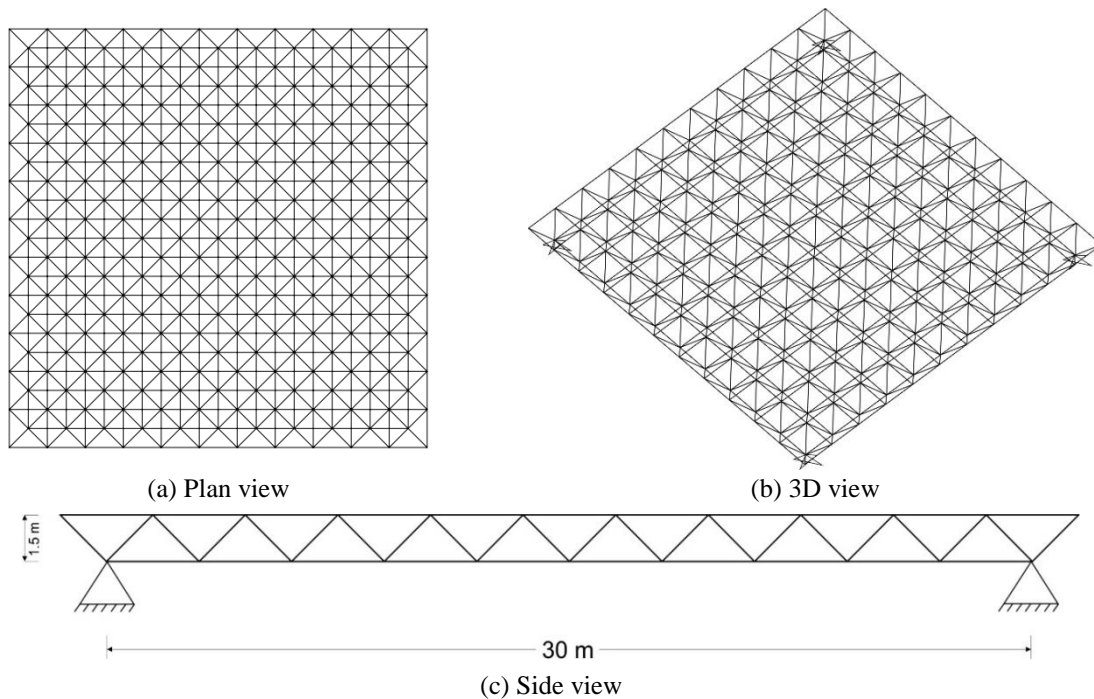

(c) Side view

Fig. 15 Schematic of a 30×30 m two-way on two-way grid

economical choice for covering small span cases. Convergence curves are compared in Fig. 13. Capacity curves are compared in Fig. 14(a) and (b). It becomes apparent that, consideration of geometric nonlinearity becomes important and it is inevitable. Through the figures, the performance of two-way on larger two-way grid is conspicuously better than diagonal on larger diagonal grid. A plot of the total forces versus displacement in diagonal on larger diagonal grid

(Fig. 14(b)) during fully nonlinear analysis would indicate the premature failure or weakness than its usual type. On the other hand, structural collapse was occurs without any noticeable change in the rate of elongation and has a little plastic deformation. Therefore, the ultimate strength and breaking strength are the same. The ultimate strength of two-way on larger two-way grid which is obtained by fully nonlinear analysis is 343 kg/m^2 while this value is equal to 303 kg/m^2 for diagonal on larger diagonal grid. It is interesting to notice that in only material nonlinear analysis two-way on larger two-way grid has better stress distribution and members are failed consecutively, for this reason the capacity curve is smooth. In the diagonal on diagonal grid some of the members are failed simultaneously whereby the stiffness of whole structure decreased abruptly at the yield point. Finally, the results completely show the superiority of two-way on larger two-way grid than diagonal on larger diagonal grid.

Example 3: *A 30× 30 m double-layer square grid*

A 30×30 m span case is considered as a big size of double-layer grids which is the last example. First common type is two-way on two-way grid which contains 265 nodes and 968 members. Second one is diagonal on diagonal grid with 401 nodes and 1520 members. Figs. 15 and 16 show the schematic of the two-way on two-way grid and diagonal on diagonal grid, respectively. Grouping pattern leads to 23 and 27 design variables for the two-way on two-way and diagonal on diagonal grid, respectively. Thus, there are two size optimization problems with 23 and 27 variables.

Element grouping is depicted in Fig. 17 in a square-like manner and due to symmetry only a quarter of the grids are shown. Table 4 in which the best obtained weight is hatched for each case
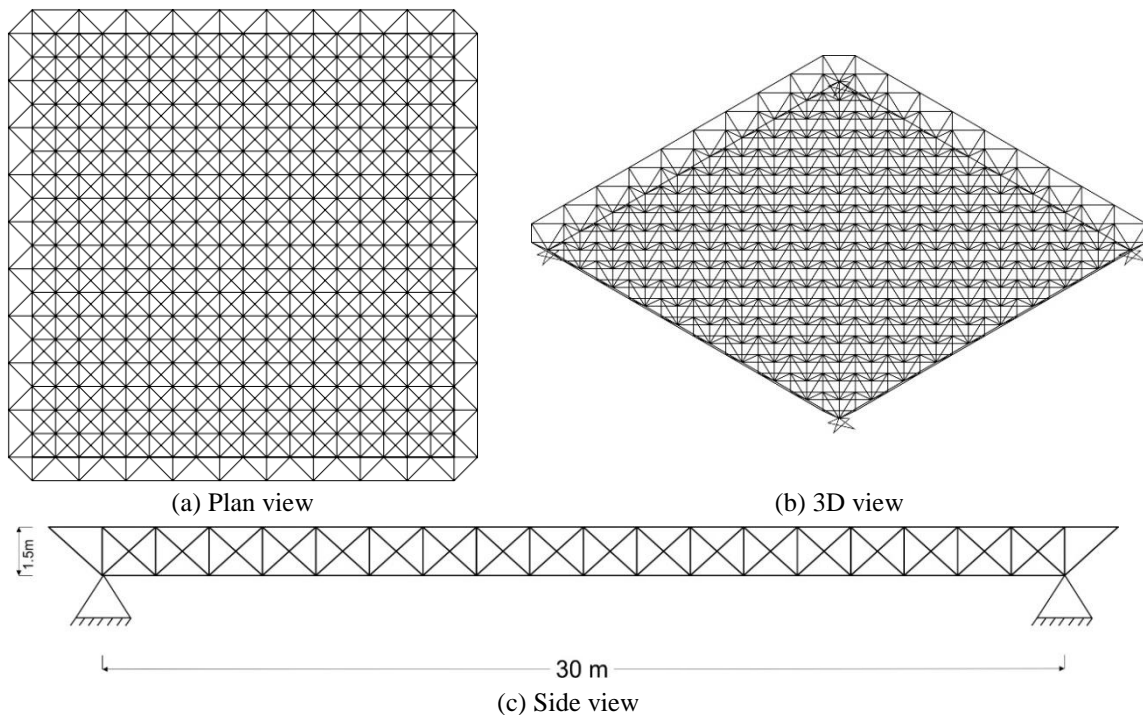

(a) Plan view   (b) 3D view

(c) Side view

Fig. 16 Schematic of a 30×30m diagonal on diagonal grid

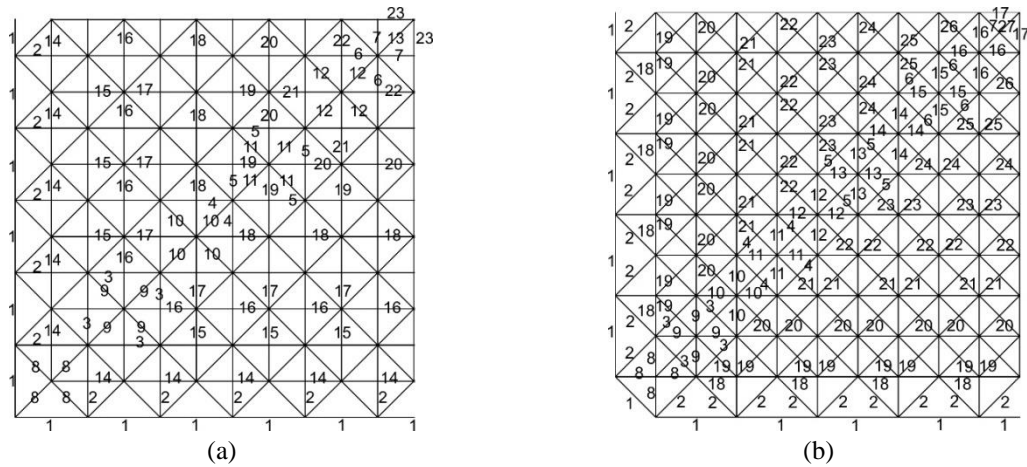(a)   (b)

Fig. 17 Element grouping of a 30×30 m (a) Two-way on two-way grid, (b) Diagonal on diagonal grid

Table 4 Optimum design of 30×30 m double-layer grids

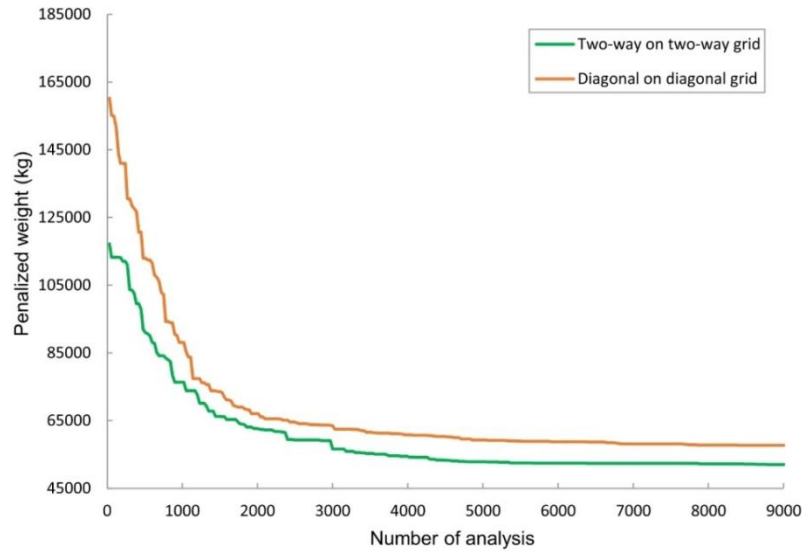| Group number	Optimum section (designations)	
	ECBO algorithm	
	Two-way on two-way grid	Diagonal on diagonal grid
1	PIPST (5)	PIPDEST (6)
2	PIPST (1)	PIPEST (3)
3	PIPEST (6)	PIPST (3)
4	PIPST (3 ½)	PIPDEST (2 ½)
5	PIPST (3 ½)	PIPST (5)
6	PIPDEST (3)	PIPEST (5)
7	PIPST (10)	PIPDEST (5)
8	PIPEST (5)	PIPST (5)
9	PIPST (3)	PIPEST (2)
10	PIPEST (2)	PIPST (2)
11	PIPEST (1 ½)	PIPEST (1 ¼)
12	PIPEST (1 ½)	PIPEST (1 ¼)
13	PIPST (1 ¼)	PIPST (1 ½)
14	PIPST (6)	PIPST (1 ½)
15	PIPEST (1 ½)	PIPST (1 ½)
16	PIPEST (4)	PIPST (1 ¼)
17	PIPST (2 ½)	PIPST (1 ½)
18	PIPDEST (2 ½)	PIPST (10)
19	PIPST (4)	PIPST (4)
20	PIPST (6)	PIPST (2 ½)
21	PIPEST (3 ½)	PIPEST (2)
22	PIPDEST (3)	PIPST (2 ½)
23	PIPEST (6)	PIPEST (2 ½)
24	N/A	PIPEST (3 ½)
25	N/A	PIPST (5)
26	N/A	PIPST (5)
27	N/A	PIPDEST (3)
Best Weight (kg)	52047.32	57683.40

Fig. 18 Convergence curves obtained for the 30×30 m double-layer grids
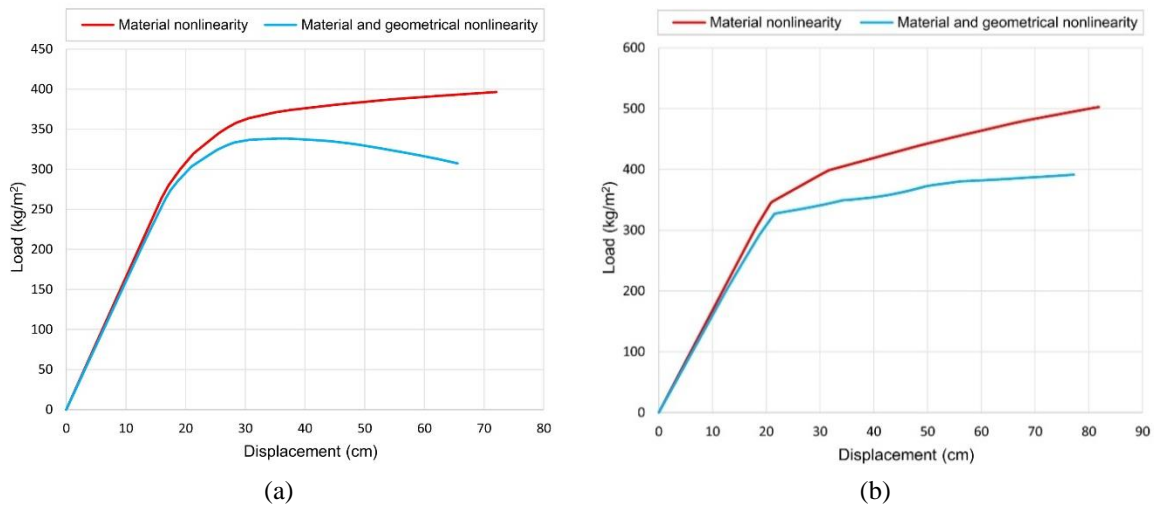

| (a) | (b) |

Fig. 19 Capacity curves of the 30×30 m (a) two-way on two-way grid, (b) diagonal on diagonal grid

presents the objective function values obtained by ECBO which are equal to 52047.32 kg and 57683.40 kg for two-way on two-way grid and diagonal on diagonal grid, respectively. In terms of the resulting low weight design in a way that the obtained optimum design for two-way on two-way grid is 9.8 percent lighter than diagonal on diagonal one. It can be realized that two-way on two-way grid is more suitable form for big span cases. Convergence history diagrams is depicted in Fig. 18. Fig. 19 shows the capacity curves for two types of grids. The fully nonlinear analysis continued up to reaching the point of total (global) collapse. The effect of geometrical nonlinearity is completely evident for two types, specially for two-way on two-way grid leads to degrading the capacity curve. It can be concluded that neglecting the geometrical nonlinear effect can be changed

the results. Therefore, considering the realistic behavior for big span cases double-layer grid is inevitable. In the comaprison of two types, two-way on two-way grid has better force distribution between members than diagonal on diagonal grid and its capacity curves are smooth while in diagonal on diagonal grid some of the elements are failed simultaneously, thereby it can be seen a fracture at the yield point during nonlinear analysis. According to the blue curves (fully nonlinear analysis) is shown in Fig. 19 the ultimate strengths are equal to 338 kg/m^2 and 391 kg/m^2 for two-way on two-way grid and diagonal on diagonal grid, respectively. Nevertheless, diagonal on diagonal grid has greater rigidity but with more number of members leads to heavier design than two-way on two-way grid.

7. Conclusions

Determining the optimum design of large-scale structure is known as one of difficult and complex optimization problems, especially when nonlinearity is taken into account. In this study, the ECBO algorithm is examined in the context of size optimization of double-layer grids designed for minimum weight. Two types of double-layer grids with various type of span length as small and big sizes are considered. Grids are designed in accordance with AISC-LRFD specification and displacement constraints. In the case of nonlinear optimization, geometrical and material nonlinearity effects are taken into account. For performance comparison, the nonlinear analysis was carried out in two phases. First only material nonlinearity is considered which is discussed as the prominent nonlinearity effects in many researches and publication. In the second phase fully nonlinear analysis is implemented. The results are indicative of the fact that in all cases two-way on two-way grid appear to be superior in the use of material to the diagonal on diagonal grid and has better stress distribution between its members. While, diagonal on diagonal grid is better than two-way on two-way grid with its greater rigidity leads to lower deflections and without considering number and complexity of joints has convenience and appealing features. In the case of square on larger square grids, two-way on larger two-way has better performance and efficiency than diagonal on larger diagonal grid with more opening parts due to its configuration has brittle behavior with a little plastic deformation. In all cases, the differences between the only material nonlinear analysis and fully nonlinear analysis are completely evident and geometrical nonlinearity has major effect during nonlinear analysis procedure. Therefore, considering the realistic behavior for double-layer grids is important and be inevitable. Results show that ECBO is an efficient and robust tool for designing large-scale problems because of the reliability of search, solution accuracy and speed of convergence.

References

American Institute of Steel Construction (AISC) (2011), "Manual of steel construction load resistance factor design", 14th Edition, AISC, Chicago, USA.

Camp, C.V., Bichon, B.J. and Stovall, S. (2005), "Design of steel frames using ant colony optimization", *J. Struct. Eng.*, ASCE, **131**, 369-379.

Code of Practice for Space Structures (2010), Publication No. 400, Technical Bureau of the Management and Planning Organization of Iran.

Degertekin, S.O. (2012), "Improved harmony search algorithms for sizing optimization of truss structures", *Comput. Struct.*, **92-93**, 229-241.

Degertekin, S.O. and Hayalioglu, M.S. (2013), "Sizing truss structures using teaching-learning based optimization", *Comput. Struct.*, **119**, 177-188.

Erbatur, F., Hasançebi, O., Tütüncü, I., and Kılıç, H. (2000), "Optimal design of planar and space structures with genetic algorithms", *Comput. Struct.*, **75**, 209-224.

Bekdaş, G., Melih Nigdeli, S. and Yang, S.S. (2015), "Sizing optimization of truss structures using flower pollination algorithm", *Appl. Soft Comput.*, **37**, 322-331.

Gholizadeh, S. (2015), "Optimal design of double layer grids considering nonlinear behavior by sequential grey wolf algorithm", *Int. J. Optim. Civil Eng.*, **5**(4), 511-523.

Gholizadeh, S. and Milany, A. (2016), "Optimal performance-based design of steel frames using advanced metaheuristics", *Asian J. Civil Eng.*, **17**, 607-623.

Gonçalves, M.S., Lopez, R.H., and Miguel, L.F.F. (2015), "Search group algorithm: a new metaheuristic method for the optimization of truss structures", *Comput. Struct.*, **153**, 165-184.

Kaveh, A. (2014), *Advances in Metaheuristic Algorithms for Optimal Design of Structures*, Springer, Switzerland.

Kaveh, A. and Forhoudi, N. (2016), "Dolphin monitoring for enhancing metaheuristic algorithms: Layout optimization of braced frames", *Comput. Struct.*, **165**, 1-9.

Kaveh, A. and Ilchi Ghazaan, M. (2014), "Enhanced colliding bodies optimization for design problems with continuous and discrete variables", *Adv. Eng. Softw.*, **77**, 66-75.

Kaveh, A. and Ilchi Ghazaan, M. (2015), "A comparative study of CBO and ECBO for optimal design of skeletal structures", *Comput. Struct.*, **153**, 137-147.

Kaveh, A. and Mahdavi, V.R. (2014), "Colliding bodies optimization: a novel meta-heuristic method", *Comput. Struct.*, **139**, 18-27.

Kaveh, A. and Mahdavi, V.R. (2015), *Colliding Bodies Optimization; Extensions and Applications*, Springer Verlag, Switzerland.

Kaveh, A. and Rezaei, M. (2015), "Optimum topology design of geometrically nonlinear suspended domes using ECBO", *Struct. Eng. Mech.*, **56**(4), 667-694.

Kaveh, A. and Talatahari, S. (2010a), "Optimal design of skeletal structures via the charged system search algorithm", *Struct. Multidiscip. Optim.* **41**, 893-911.

Kaveh, A. and Talatahari, S. (2010b), "Optimal design of Schwedler and ribbed domes via hybrid Big Bang Big Crunch algorithm", *J. Construct. Steel Res.*, **66**, 412-419.

Kaveh, A. and Talatahari, S. (2011), "Geometry and topology optimization of geodesic domes using charged system search", *Struct. Multidiscip. Optim.* **43**:215-229.

Koushky, A.L., Dehdashti, G. and Fiouz, A. (2009), "Nonlinear analysis of double-layer grids with compositive nodes under symmetric and unsymmetrical gravity loads", *Int. J. Space Struct.*, **22**(2), 133-140

Makowski, Z.S. (1990), *Analysis, design and construction of double-layer grids*, Applied Science Publisher Ltd, London.

Mirjalili, S. (2015), "The ant lion optimizer", *Adv. Eng. Softw.*, **83**, 80-98.

OpenSees. (2011), Open System for Earthquake Engineering Simulation, Pacific Earthquake Engineering research Center, University of California.

Perez, R.E. and Behdinan, K. (2007), "Particle swarm approach for structural design optimization", *Comput. Struct.*, **85**, 1579-1588.

Sadollah, A., Eskandar, H., Bahreininejad, A. and Kim, J.H. (2015), "Water cycle, mine blast and improved mine blast algorithms for discrete sizing optimization of truss structures", *Comput. Struct.*, **149**, 1-16.

Saka, M.P. (2007), "Optimum geometry design of geodesic domes using harmony search algorithm", *Adv. Struct. Eng.*, **10**(6), 595-606.

Saka, M.P. and Ulker, M. (1991), "Optimum design of geometrically nonlinear space trusses", *Comput. Struct.*, **41**, 1387-1396.

CC